The Radiometric Bode's Law and Extrasolar Planets

T. Joseph W. Lazio

Naval Research Laboratory, Code 7213, Washington, DC 20375-5351

Joseph.Lazio@nrl.navy.mil

W. M. Farrell

NASA Goddard Space Flight Center, Code 695, Greenbelt, MD 20771

william.m.farrell@gsfc.nasa.gov

Jill Dietrick, Elizabeth Greenlees, Emily Hogan, Christopher Jones, L. A. Hennig

Thomas Jefferson High School for Science and Technology, 6650 Braddock Road, Alexandria, VA 22312

hennig@lan.tjhsst.edu

ABSTRACT

We predict the radio flux densities of the extrasolar planets in the current census, making use of an empirical relation—the radiometric Bode's Law—determined from the five "magnetic" planets in the solar system (Earth and the four gas giants). Radio emission from these planets results from solar-wind powered electron currents depositing energy in the magnetic polar regions. We find that most of the known extrasolar planets should emit in the frequency range 10–1000 MHz and, under favorable circumstances, have typical flux densities as large as 1 mJy. We also describe an initial, systematic effort to search for radio emission in low radio frequency images acquired with the Very Large Array. The limits set by the VLA images (≈ 300 mJy) are consistent with, but do not provide strong constraints on, the predictions of the model. Future radio telescopes, such as the Low Frequency Array (LOFAR) and the Square Kilometer Array (SKA), should be able to detect the known extrasolar planets or place austere limits on their radio emission. Planets with masses much lower than those in the current census will probably radiate below 10 MHz and will require a space-based array.

1. Introduction

The past few years have been an exciting time as extrasolar planets have been demonstrated to be widespread and multiple planetary systems have been found. The current census now numbers more than 100 extrasolar planets, in over 90 planetary systems (Schneider 2003; Marcy 2003).

The vast majority of these extrasolar planets have been detected via the reflex motion of the host star. As the existing census shows, this method has proven to be wildly successful. Nonetheless, the reflex motion of the star is a measure of the planet's gravitational influence and is necessarily an *indirect* detection of the planet. As a consequence, the only property of the planet that one can infer is its mass, and because of the mass function's dependence on the inclination angle ($\sin i$), one can infer only a minimum mass.

Direct detection of reflected, absorbed, or emitted radiation from a planet allows for the possibility of complementary information, and likely a more complete characterization of the planet. The prototype of such a direct detection is the detection of sodium absorption lines in the atmosphere of the planet orbiting HD 209458 (Charbonneau et al. 2002). Unfortunately, the incidence of transiting planets will always remain low relative to the total number of planets known.

The Earth and gas giants of our solar system are described commonly as "magnetic planets" because they contain internal dynamo currents that are capable of generating a planetary-scale magnetic field. The dynamo currents themselves arise from the rapid rotation of a conducting fluid. The composition of the fluid varies from planet to planet, being liquid iron in the Earth, probably metallic hydrogen in Jupiter and Saturn, and probably a salty ocean in Uranus and Neptune. In turn, these planetary magnetic fields are immersed in the high-speed electrical gas emitted by the Sun. Via a coupling between the solar wind and the planetary magnetic field, all of these magnetic planets produce radio emission.

Some of the extrasolar planets are also magnetic planets. Shkolnik, Walker, & Bohlender (2003) have detected a modulation in the Ca II H and K lines of HD 179949 with a periodicity which is that of the planetary orbit. They interpret this as a magnetic interaction between the star and planet, though there is no constraint as yet on the magnetic field strength of the planet. Other stars in their sample also appear to have modulations in the Ca II H and K lines, though it is not yet clear that these modulations are periodic with the orbital period of their planets, as is the case for HD 179949.

By analogy to solar system planets, there have been a number of suggestions and searches for natural radio emission from extrasolar planets. Early searches were conducted by Yantis, Sullivan, & Erickson (1977) and Lecacheux (1991). Due to the lack of any known extrasolar planets at the time, these were necessarily blind searches. More recently, Farrell, Desch, & Zarka (1999) and Zarka et al. (2001), building on empirical relations derived for solar system planets and calibrated by spacecraft fly-bys, have made specific predictions for the radio emission from the known extrasolar planets.

Detection of radio emission from an extrasolar planet would constitute a *direct* detection and can yield fundamental information about the planet. First, a measurement of the radio emission is directly indicative of the polar magnetic field strength at the planet. For example, the high-frequency cutoff of Jovian decametric bursts ($\simeq 40$ MHz) is interpreted as being due to the Jovian polar magnetic field strength, which allowed an estimate for the strength of the Jovian magnetic

field nearly 20 yr prior to the first *in situ* magnetic field observations. In turn, of course, the presence of a magnetic field provides a rough measure of the composition of the planet, insofar as it requires the planet's interior to have a conducting fluid. Combined with an estimate of the planet's mass, one could deduce the composition of the fluid by analogy to the solar system planets (liquid iron vs. metallic hydrogen vs. salty ocean).

Second, the periodic nature of the radio emission has been used to define precisely the planetary rotation periods of all of the gas giant planets in the solar system. As the magnetic field is presumed to be tied to the interior of the planet, it provides a more accurate measure of the planet's rotation rate than atmospheric phenomena such as clouds. For instance, the rotation period of Neptune was determined initially by observations of the differentially rotating cloud tops but then was redefined after detection of the Neptunian radio emission (Lecacheux et al. 1993).

Finally, testing the extent to which solar-system models of magnetic fields can be applied to extrasolar planets may have important implications for assessing the long-term "habitability" of any terrestrial planets found in the future. The importance of a magnetic field is that it deflects incident cosmic rays. If these particles reach the surface of an otherwise habitable planet, they may cause severe cellular damage and disruption of genetic material to any life on its surface or may prevent life from arising at all. A secondary importance of a magnetic field is that it can prevent the planet's atmosphere from being eroded by the stellar wind (Mitchell et al. 2001); this process is thought to be a contributing factor to the relative thinness of the Martian atmosphere. (This is of course unlikely to be an issue for extrasolar giant planets.)

This paper extends and updates initial attempts to predict the radio emission of extrasolar giant planets by applying the solar-system determined "radiometric Bode's Law" to the current census of extrasolar planets. In §2 we summarize briefly the various forms of the radiometric Bode's Law and the form we have adopted for use, in §3 we summarize the current state of the extrasolar planet census and predict the "burst" emission levels and frequencies for radio emission from these planets, in §4 we use the initial observations from a 74 MHz sky survey to confront the model predictions with data, and in §5 we assess how existing and future radio telescopes may be able to detect radio emission from extrasolar planets and present our conclusions.

2. The Radiometric Bode's Law

All of the planets in the solar system with substantial magnetic fields are strong emitters of coherent cyclotron emission at radio wavelengths. The emission itself arises from energetic (keV) electrons propagating along magnetic field lines into active auroral regions (Gurnett 1974; Wu & Lee 1979). The source of the electron acceleration to high energies is ultimately a coupling between the incident solar wind and the planet's magnetic field. The precise details are not well understood, but the coupling arises from magnetic field reconnection in which the magnetic field embedded in the solar wind and the planetary magnetic field cancel at their interface, thereby energizing the

plasma. Energetic electrons in the energized plasma form a current flow planet-ward along the planet's magnetic field lines, with the lines acting effectively like low resistance wires. The energy in these magnetic field-aligned electric currents is deposited in the upper polar atmosphere and is responsible for the visible aurora. Besides auroral emissions at visible wavelengths (e.g., northern lights), about 10^{-5}–10^{-6} of the solar wind input power is converted to escaping cyclotron radio emission (Gurnett 1974). The auroral radio power from Earth is of order 10^8 W while for Jupiter it is of order $10^{10.5}$ W.

The cyclotron emission process described is generic, and typically most efficient in the auroral region, about 1–3 planetary radii in altitude. Specific details of the cyclotron emission process do differ from planet to planet, depending upon secondary effects such as the polar source location and beaming angles, which in turn depend upon the planet's magnetic field topology and low-altitude atmospheric density. Nonetheless, applicable to all of the magnetic planets is a macroscopic relationship called the "radiometric Bode's law" relating the incident solar wind power, the planet's magnetic field strength, and the median emitted radio power. Various investigators (Desch & Barrow 1984; Desch & Kaiser 1984; Desch & Rucker 1985; Barrow, Genova, & Desch 1986; Rucker 1987; Desch 1988; Millon & Goertz 1988) have found

$$P_{\mathrm{rad}} = \epsilon P_{\mathrm{sw}}^x, \tag{1}$$

where P_{rad} is the median emitted radio power, P_{sw} is the incident solar wind power, $\epsilon \sim 10^{-5}$–10^{-6} is the efficiency at which the solar wind power is converted to emitted radio power, and $x \approx 1$. The values of the coefficient ϵ and the power-law index x measured by various investigators have differed over the years based on the quantity of data available; the early determinations were based on fly-bys of only Jupiter and Saturn and measurements of the Earth's radio emission while later determinations include data from the Voyager 2 Uranus and Neptune fly-bys as well. In general, the more recent work indicates higher efficiencies than the earlier work (Zarka et al. 1997).

Farrell et al. (1999) and Zarka et al. (2001) extrapolated this relation to extrasolar planetary systems by making use of two scaling relations and adopting more recent estimates for ϵ and x. The incident solar wind power depends upon the ram pressure of the solar wind and the cross-sectional area presented by the magnetosphere to the solar wind. The ram pressure of the solar wind depends on the star-planet distance d while the size of the planet's magnetosphere is related to its magnetic moment. Blackett (1947) demonstrated that planetary-scale, dynamo-driven magnetic fields are scalable, with a functional dependence on body mass, radius, and angular frequency; and the presence of planetary-scale magnetic fields around the gas giants shows that his analysis does not depend upon the actual composition of the conducting fluid in the planet's interior. Blackett's law relates a planet's magnetic moment (its surface field times its radius cubed, BR^3) to its rotation rate and mass by

$$\mu \sim \omega M^2, \tag{2}$$

where ω is the planet's rotation rate and M is its mass. Since that time and with the inclusion of the Voyager magnetic field observations at the outer planets, numerous planetary magnetic field

scaling laws have been derived, each expanding upon but maintaining some similarity to Blackett's Law.

Combining these various scaling relations, Farrell et al. (1999) and Zarka et al. (2001) found that the planet's median radio power driven by the stellar wind is

$$P_{\rm rad} \sim 4 \times 10^{11}\,{\rm W} \left(\frac{\omega}{10\,{\rm hr}}\right)^{0.79} \left(\frac{M}{M_J}\right)^{1.33} \left(\frac{d}{5\,{\rm AU}}\right)^{-1.6}. \tag{3}$$

We have normalized all quantities to those of Jupiter. Farrell et al. (1999, Appendix A) discussed slight differences to this radiometric Bode's law, the differences result from the statistical spread in the various (solar system) planets' magnetic moments and amount to slightly different exponents and/or a different coefficient.

We stress various aspects of this radiometric Bode's law. First, it is grounded in *in situ* measurements from spacecraft fly-bys of the gas giants as well as measurements of the Earth's radio emission. In particular, Farrell et al. (1999) considered two forms of the radiometric Bode's Law, one incorporating measurements of only Jupiter and Saturn and the other incorporating all five magnetic planets. The former gives lower power levels (by a factor of 100); in equation (3), we have adopted the latter because it is based on a complete census of magnetic planets in the solar system.

Second is the importance of the planet-star distance. As Zarka et al. (2001) show, the radio power from Earth is larger than that from Uranus or Neptune even though both of those planets have magnetic moments approximately 50 times larger than that of the Earth.

Third, the power levels estimated by equation (3) are for emission into a solid angle of 4π. Emission solid angles for solar system planets span a large range. Considering Jovian decametric emission at macroscopic scales, emission occurrence is as $\Omega \sim \pi$. In estimating the flux density, the relevant quantity is P/Ω. (See equation 5 below and the discussion in Farrell et al. 1999.) Assuming a smaller emission solid angle would mean reducing the nominal power levels of equation (3) by the factor $\Omega/4\pi$. (This factor also explains the difference between the nominal power level for Jupiter predicted by equation 3 and the level quoted in §1.)

Fourth, the radiometric Bode's Law of equation (3) describes the *median* emitted power from the magnetospheres of the Earth and all of the solar gas giants, including the *non-Io driven* Jovian decametric radio emission (Zarka et al. 2001). Planetary magnetospheres tend to act as "amplifiers" of the incident solar wind, so that an increase in the solar wind velocity (and therefore incident pressure) leads to geometrically higher emission levels. This effect is observed at all of the magnetized planets. For instance, the Saturnian radio flux has been observed to increase by factors of 20 due to changes in the solar wind velocity (Desch & Rucker 1985). At the Earth, the radio power has been observed to increase by a factor of 10 for every 200 km s^{-1} increase in the solar wind velocity (Gallagher & D'Angelo 1981, Figure 5); the observed range of solar wind velocities at the Earth is at least 400 km s^{-1} (from 400 km s^{-1} to 800 km s^{-1}). The radio power levels from a planet can exceed that predicted by equation (3) by factors of 100 and possibly more.

Finally, an implicit assumption in our analysis is that the mass loss rates for stars hosting planets are similar to that of the Sun. The stellar wind pressure incident on a planetary magnetosphere is $P_{\rm sw} \propto \rho V^3$, where ρ is the density of the stellar wind and V is its velocity. Stars with higher (lower) mass loss rates than the Sun will have higher (lower) stellar wind densities and should drive higher (lower) planetary radio emissions. Differences in the mass loss rate from star to star could lead to statistical variations in the power levels we predict, though these should be relatively less important than variability in stellar wind velocities. (Work is in progress to utilize what is known about the various stellar ages and activities to relax this assumption.)

In order for gyrating electrons to generate radio emission that escapes the auroral region, the Doppler-shifted electron cyclotron frequency must couple directly to a magnetoplasma mode. This coupling can only occur in low density, high magnetic field conditions where the local electron plasma-to-cyclotron frequency ratio is much less than one. The regions just above the polar ionosphere satisfy this coupling criteria. Hence, the characteristic emission frequency can be related to the planetary magnetic dipole moment (equation 2) by

$$\nu_c \sim 23.5 \, {\rm MHz} \, \left(\frac{\omega}{\omega_J}\right) \left(\frac{M}{M_J}\right)^{5/3} R_J^3. \tag{4}$$

In order to be detected from ground-based telescopes, ν_c must exceed the terrestrial ionospheric cutoff (defined by the peak ionospheric plasma frequency), which is typically 3–10 MHz. Farrell et al. (1999) showed that ν_c exceeded the Earth's ionospheric cutoff (~ 3 MHz) for some planets known at the time of the publication of their paper, with the planet around HD 114762 having $\nu_c \approx 1000$ MHz.

Just as the statistical variations in the solar-system planetary magnetic moments contribute to variations in the radiometric Bode's Law, there is also a statistical spread in the exponents and/or coefficients for the emission frequency. Compared to the radiated power predicted by equation (3), the statistical variations in the predicted emission frequency are relatively more important. The radiated power levels can be exponentially modified by the solar-wind loading whereas the emission frequency is not. In order to account for the statistical variations in estimates of the magnetic moment derived from Blackett's Law, we assume that the actual emission frequency could be larger or smaller by a factor of 3 than the nominal value of equation (4). (See also Appendix A of Farrell et al. 1999.)

The predicted flux density of an extrasolar planet is then

$$S = \frac{P}{\Delta \nu \Omega D^2}. \tag{5}$$

Farrell et al. (1999) applied equations (2)–(5) to the nine then-known extrasolar planets. The distances to the host stars are known. The planetary mass and distance to its parent star are measured or constrained from the optical observations. Assuming an emission cone of 4π sr, $\Delta \nu = \nu_c/2$, and a rotation rate comparable to that of Jupiter, they derived the resulting flux densities.

We shall do the same but for the currently much larger sample.

3. The Extrasolar Planet Census

Since the initial work by Farrell et al. (1999), the extrasolar planetary census has grown by over an order of magnitude. We used the census of extrasolar planets contained in "The Extrasolar Planets Encyclopaedia" (Schneider 2003). We used only the set of reasonably secure detections of planets around main-sequence stars as of 2003 July 1. The total number of planets examined was 118 in 102 planetary systems.

The required quantities for applying equation (3) are the planet's mass, distance from its primary, and rotation rate. At the time we extracted our list of planets from "The Extrasolar Planets Encyclopaedia," almost all of the known planets had been found via the radial velocity method. This method yields a lower limit to the planet's mass (i.e., $M \sin i$).

Strictly, with the exception of the planets orbiting OGLE-TR-56 and HD 209458, for which transits have been detected, the flux density levels that we calculate are lower limits. If the emitted radiation is nearly isotropic and assuming that the inclinations of the orbits are random, the typical error introduced is only a factor of 2. There have been attempts to set upper limits on planetary masses, e.g., using tidal constraints (Trilling 2000). We have not made use of these upper limits because in many cases they introduce additional uncertainties based on the characteristics of the host star (e.g., its age).

The radial velocity method also determines the semi-major axis and eccentricity of the planet's orbit. We use the semi-major axis as the distance d in equation (3). For those planets in eccentric orbits, we might expect the radio emission to be periodic with the planet's orbital period, increasing near periastron and decreasing near apastron. The most extreme eccentricities in our sample are approximately 0.7 (HIP 75458, HD 222582, and HD 2039). We therefore expect a range of possible flux densities of possibly 20. For a planet with a more typical eccentricity, $e \approx 0.1$, the range is only a factor of 1.5 or so.

We have no information on the rotation rates of these planets. We have therefore assumed that those planets with semi-major axes larger than 0.1 AU have rotation rates equal to that of Jupiter (10 hr), while those with semi-major axes less than 0.1 AU are tidally-locked with rotation rates equal to their orbital periods (Goldreich & Soter 1966; Trilling 2000).

For tidally-locked planets we have also assumed a radius of 1.25 R_J in calculating the characteristic frequency. This value is both predicted based on the stellar insolation of such planets (Guillot et al. 1996) and is close to the observed value for the planet orbiting HD 209458 (Charbonneau et al. 2002).

Table 1 presents the full list of planets in our sample along with the expected emission frequencies and flux density levels. Figure 1 presents the expected flux densities vs. the emission frequency

in a graphical form. Anticipating our analysis of §4, we follow the convention of Farrell et al. (1999) and increase the predicted flux density levels by a factor of 100 in order to account for variability driven by the incident stellar wind.

Table 1.   Exoplanet Radio Emission

Star	ω/ω_J	$\log P_{\rm rad}$ (W)	μ (G R$_J$)	ν_c (MHz)	$\log S$ (Jy)
OGLE-TR-56	0.3	16.95	2.6	14.8	−4.3
HD 73256	0.2	16.77	3.7	20.8	−1.4
HD 83443	0.1	15.79	0.3	1.4	−1.4
HD 46375	0.1	15.48	0.1	0.6	−1.1
HD 179949	0.1	16.28	1.1	5.9	−1.1
HD 187123 b	0.1	15.88	0.4	2.1	−1.6
HD 209458	0.1	15.95	0.5	2.9	−1.6
HD 75289	0.1	15.65	0.2	1.3	−1.2
BD −10° 3166	0.1	15.73	0.3	1.6	$\cdots$
HD 76700	0.1	15.13	0.1	0.3	−1.7
τ Boo	0.1	16.93	10.7	59.9	−1.0
51 Peg	0.1	15.57	0.2	1.2	−0.6
HD 49674	0.1	14.66	0.0	0.1	−1.4
υ And b	0.09	15.67	0.4	2.2	−0.7
υ And c	1.0	15.25	12.1	68.0	−2.6
υ And d	1.0	14.87	38.0	213	−3.5
HD 168746	0.07	14.86	0.0	0.3	−1.6
HD 217107 b	0.06	15.76	0.7	4.0	−1.8
HD 68988	0.07	16.02	1.6	8.8	−2.2
HD 162020	0.05	17.06	31.7	178	−2.0
HD 130322	0.04	15.36	0.4	2.0	−1.7
HD 108147	0.04	14.67	0.1	0.4	−1.8
Gl 86	1	17.08	42.3	237	−1.2
55 Cnc b	1	16.15	3.1	17.6	−1.1
55 Cnc c	1	14.84	0.3	1.7	−1.4
55 Cnc d	1	14.32	43.2	242	−4.1
HD 38529 b	1	16.03	2.8	15.5	−2.2
HD 38529 c	1	15.31	290.4	1626	−4.9
HD 195019	1	16.83	32.8	184	−1.8
HD 6434	1	15.64	1.2	6.9	−2.2
HD 192263	1	15.88	2.4	13.6	−1.6

Table 1—Continued

Star	ω/ω_J	$\log P_{\rm rad}$ (W)	μ (G R$_J$)	ν_c (MHz)	$\log S$ (Jy)
Gl 876 b	1	16.20	12.1	68.0	−0.8
Gl 876 c	1	15.83	1.6	8.9	−0.2
ρ CrB	1	15.82	4.9	27.6	−1.8
HD 74156 b	1	15.90	8.8	49.4	−3.2
HD 74156 c	1	15.05	120.7	676	−5.2
HD 3651	1	14.69	0.3	1.6	−1.4
HD 168443 b	1	16.75	112.8	631	−2.9
HD 168443 c	1	15.66	476.7	2670	−4.6
HD 121504	1	15.47	3.5	19.4	−2.9
HD 178911B	1	16.60	90.1	504.4	−3.2
HD 16141	1	14.59	0.3	1.8	−2.6
70 Vir	1	16.42	97.5	546	−2.8
HD 80606	1	16.03	32.4	182	−3.5
HD 219542B	1	14.59	0.6	3.2	−3.2
HD 216770	1	15.08	2.3	13.0	−3.0
GJ 3021	1	15.94	31.0	174	−2.6
HD 52265	1	15.31	5.1	28.8	−2.8
HD 37124 b	1	15.01	2.6	14.6	−3.0
HD 37124 c	1	14.22	5.7	31.9	−4.1
HD 73526	1	15.67	26.2	147	−4.3
HD 8574	1	15.40	16.0	89.5	−3.6
HD 104985	1	15.98	90.3	505	−4.5
HD 134987	1	15.18	9.0	50.4	−3.1
HD 169830 b	1	15.51	23.5	132	−3.5
HD 169830 c	1	14.53	17.2	96.3	−4.3
HD 40979	1	15.59	31.0	174	−3.5
HD 150706	1	14.89	4.2	23.5	−3.1
HD 12661 b	1	15.36	16.8	94.3	−3.5
HD 12661 c	1	14.35	8.9	49.9	−4.3
HD 89744	1	15.98	112.8	631	−3.8
HR 810	1	15.27	16.2	90.9	−2.8

Table 1—Continued

Star	ω/ω_J	$\log P_{\rm rad}$ (W)	μ $({\rm G\,R}_J)$	ν_c (MHz)	$\log S$ (Jy)
HD 92788	1	15.56	39.5	221	−3.6
HD 142	1	14.76	4.2	23.5	−3.0
HD 177830	1	14.89	6.3	35.5	−4.0
HD 128311	1	15.30	21.0	118	−3.0
HD 28185	1	15.73	76.4	428	−3.9
HD 108874	1	14.99	9.7	54.2	−4.2
HD 142415	1	15.02	10.5	58.6	−3.6
HD 4203	1	14.97	9.6	53.6	−4.3
HD 210277	1	14.81	6.0	33.7	−3.2
HD 82943 b	1	14.93	9.5	53.1	−3.5
HD 82943 c	1	14.89	3.4	19.0	−3.0
HD 27442	1	14.84	7.6	42.7	−3.1
HD 114783	1	14.61	4.1	23.1	−3.2
HD 20367	1	14.63	4.7	26.3	−3.4
HD 147513	1	14.59	4.2	23.5	−2.8
HD 19994	1	14.97	13.3	74.7	−3.4
HD 65216	1	14.73	6.8	37.8	−3.7
HD 41004A	1	15.04	16.8	94.3	−4.0
HIP 75458	1	15.79	152.8	856	−3.9
HD 222582	1	15.48	63.7	357	−4.1
HD 160691	1	14.78	10.2	57.0	−3.1
HD 23079	1	15.01	19.9	111	−3.9
HD 141937	1	15.77	185.3	1038	−4.1
HD 47536	1	15.34	60.6	339	−5.1
HD 114386	1	14.41	4.1	23.1	−3.6
HD 4208	1	14.26	3.0	16.6	−3.8
16 Cyg B	1	14.61	8.3	46.2	−3.5
HD 10697	1	15.36	97.3	545	−4.1
γ Cep	1	14.52	9.1	50.9	−3.1
HD 213240	1	15.12	51.5	289	−4.3
HD 111232	1	15.43	128.8	722	−4.1

The trend in Figure 1 of increasing emission frequency and decreasing flux density is real and reflects two effects. First, the lower envelope reflects a selection effect. A low flux density and small emission frequency results from a low-mass planet in a large orbit. These planets cannot be detected with the current detection methodology. Second, the upper envelope reflects the well-known deficit of planets with both large masses and small semi-major axes. Even if high-mass planets with close orbits did exist, however, they probably would be tidally locked (as we have assumed here). The rotation rate also determines the strength of the magnetic field (equation 4), so tidally-locked planets probably do not radiate at high emission frequencies. However, Zarka et al. (2003) have suggested that such "hot Jupiters" may radiate by the conversion of stellar magnetic pressure (which is large in close to the star) into electromotive forces, currents and radio emission.

We have assumed that the objects discussed here (Table 1) are in fact planets. Using Hipparcos astrometric data, Han, Black, & Gatewood (2001) argue that the inclinations of the orbits of these objects imply that $\sin i$ is small. A small $\sin i$ would imply that the derived masses of these objects would be larger, so that their magnetic moments would be larger, but also that their distances from their stars would be larger, so that the stellar wind loading of the magnetosphere would be less. The similar dependences for M and d in equation (3) mean that this impact of small $\sin i$ would nearly cancel. However, if $\sin i$ is small enough, as Han et al. (2001) suggest for a number of objects, they might no longer be classified as planets but as brown dwarfs. Berger et al. (2001) detected radio emission from one brown dwarf, indicating that it is likely to be a magnetic body as well. If so, the radiometric Bode's Law and our analysis might still apply to them.

We now discuss selected objects in greater detail.

OGLE-TR-56 The planet orbiting this star was found from its transits of its parent star (Konacki et al. 2003). In many respects it is not much different than many of the other "close-in" planets. Its flux density is roughly 3 orders of magnitude lower, though, because of its much greater distance (1500 pc vs. a more typical 10 pc). This result is likely to be a general result as future planetary searches move deeper into the Galaxy: The detection of extrasolar planetary radio emission is most likely to come from planets orbiting nearby stars.

HD 179949 A possible magnetic interaction between the planet and the star has been detected for this star (Shkolnik et al. 2003).

τ Boo, HD 209458 These stars show Ca II H and K activity, similar to that of HD 179949. However, a clear link between the planetary orbital period and the modulation of the Ca II H and K emission has not been established yet (Shkolnik et al. 2003).

HD 187123 This star may have (at least) two planets orbiting it (Vogt et al. 2000). We provide a prediction for only the inner planet. The outer planet has a period much longer than 3 yr. Consistent with other planets having relatively long periods ($d \sim 2\ AU$), we would expect the flux density from this second planet to be no more than about 10^{-5} Jy.

Table 1—Continued

Star	ω/ω_J	$\log P_{\rm rad}$ (W)	μ (G R_J)	ν_c (MHz)	$\log S$ (Jy)
HD 114729	1	14.12	3.0	16.9	−4.0
47 UMa b	1	14.77	19.9	111	−3.3
47 UMa c	1	13.67	2.7	14.9	−3.5
HD 10647	1	14.32	5.5	30.6	−3.4
HD 2039	1	15.14	63.5	355	−5.1
HD 190228	1	15.09	61.2	343	−4.9
HD 50554	1	15.06	59.4	333	−4.2
HD 136118	1	15.57	260.9	1461	−4.8
HD 196050	1	14.75	26.2	147	−4.5
HD 30177	1	15.26	126.1	706	−4.8
HD 106252	1	15.19	102.8	576	−4.5
HD 216435	1	14.29	8.2	45.7	−4.2
HD 216437	1	14.49	14.5	81.0	−4.0
HD 23596	1	15.19	112.5	630	−4.8
14 Her	1	14.94	59.4	333	−3.9
HD 72659	1	14.47	20.0	112	−4.8
ϵ Eri	1	13.83	3.3	18.3	−2.2
HD 39091	1	15.26	204.8	1147	−4.2
HD 33636	1	15.39	183.4	1027	−4.3
Gl 777A	1	13.82	6.8	37.8	−3.9

Note. — Planets are arranged roughly in order of increasing semi-major axis. The predicted flux densities are the burst values.
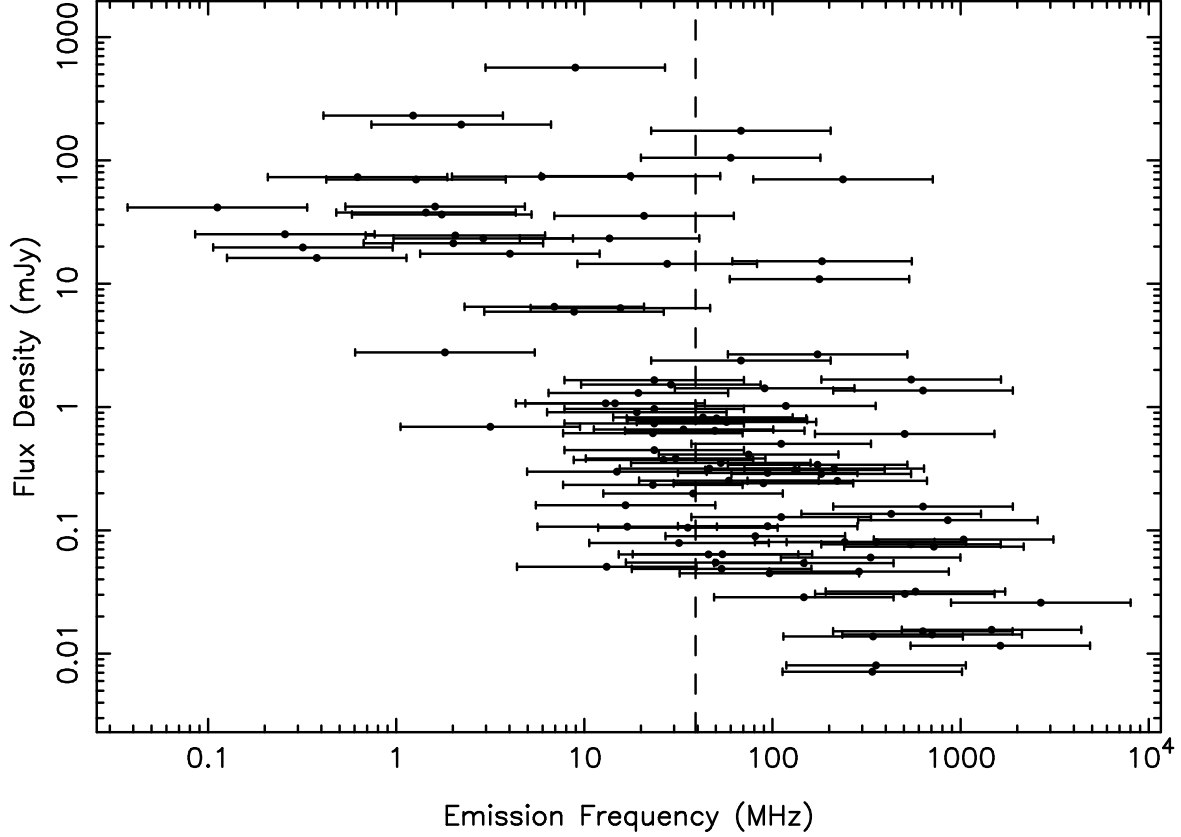
Fig. 1.— The predicted "burst" flux densities for 106 known extrasolar planets vs. the characteristic emission frequency based on the radiometric Bode's Law and Blackett's Law, equations (3)–(5). The horizontal bars indicate the assumed ranges for the emission frequencies, allowing the statistical variations from Blackett's Law in the estimated planetary magnetic moments. The expected *burst* flux densities are obtained by assuming that increases of roughly a factor of 100 can be obtained by larger stellar wind loading of the planet's magnetosphere. The vertical dashed line indicates the approximate cutoff frequency for Jupiter.

BD $-10°$ **3166** This star has a planet orbiting it, but the distance to the star is unknown, though Butler et al. (2000) suggest a distance of less than 200 pc. If that is the case, its flux density is probably larger than 10^{-3} Jy.

υ **And** There is uncertainty regarding the mass of the outer planet, with Butler et al. (1999) finding 4.6 M$_J$ while Mazeh et al. (1999) find approximately 10 M$_J$. We have used the lower value, realizing that this factor of two difference results in only a modest change in both ν_c and S.

This star also shows Ca II H and K activity, similar to that of HD 179949. However, a clear link between the planetary orbital period and the modulation of the Ca II H and K emission has not been established yet (Shkolnik et al. 2003).

HD 217107 This star may have (at least) two planets orbiting it (Fischer et al. 2001). We provide a prediction for only the inner planet. The outer planet has a period much longer than 3 yr. Consistent with other planets having relatively long periods ($d \sim 2\ AU$), we would expect the flux density from this second planet to be no more than about 10^{-5} Jy.

HD 74156 The mass of the outer planet orbiting this star is uncertain (in addition to the inclination factor). The cited lower limit is 7.5 M$_J$. A larger value would lead to both a higher ν_c and S.

HD 92788 Estimates of the mass of the planet orbiting this star differ by 5% (Udry, Mayor, & Queloz 2000; Fischer et al. 2001). We have used the arithmetic mean of the masses and semi-major axis in estimating the flux density.

HD 160691 The existing radial velocity data indicate, though do not provide a compelling case, for the presence of an outer planet (Jones et al. 2002). If this second planet does exist, its predicted magnetic moment and radio emission would be similar to those of HD 216435.

ϵ **Eri** Quillen & Thorndike (2002) claim the presence of an outer planet based on the structure of the dust disk surrounding this star. Even if such a planet exists, its large semi-major axis (≈ 40 AU) would imply that its radio emission would be similar to that of Neptune, almost certainly at a frequency well below the Earth's ionospheric cutoff.

HD 192263 The existence of a planet around this star was questioned on the basis of photometric variations with the same period as the radial velocity variations (Henry, Donahue, & Baliunas 2003). Santos et al. (2003) present more recent radial velocity measurements, which appear to confirm the presence of the planet.

HD 47536 The mass of the star is uncertain and in the range 1–3 M$_\odot$ (Setiawan et al. 2001). We have used the lower limit to obtain the mass of the planet. Adopting a larger mass would imply a larger predicted flux density, by a factor of as much as 4.

The star itself is a giant (spectral class K1III). As the radiometric Bode's Law was developed for planets orbiting a main-sequence star, whether it can be applied to planets orbiting giant stars is not clear.

HD 114762 This object does not appear in Table 1, even though Farrell et al. (1999) made a prediction for its radio emission, because it has since been re-classified as a brown dwarf (Schneider 2003). Radio emission may still be generated from such bodies, though (Berger et al. 2001).

4. VLA 74 MHz Observations: An Initial Comparison

The model presented represents a zeroth-order estimate under the assumption that a solar analog is valid. To confirm or refute the model some initial confrontation with observations is warranted, even if the observations cannot be obtained "optimally" in some sense. For this purpose we utilize the VLA Low-frequency Sky Survey (VLSS), an effort to survey the northern sky using the VLA's 74 MHz system (Kassim et al. 2003). We make use of this survey for two reasons. First, at a frequency of 74 MHz, the survey frequency is within a factor of 2 of the cutoff frequency of the radio emission of Jupiter ($\simeq$ 40 MHz) and within a factor of 2 of the predicted emission frequencies for nearly one-third of the current census.

Second, in producing Table 1 we have reported "burst" flux densities, which are a factor of 100 larger than the median values. Our rationale for doing so is that we occasionally may detect the bursts from extrasolar planets. The VLSS observations are a series of overlapping pointing centers on the sky with each pointing center observed in five, 15-min. "snapshots." While not as sensitive as the targeted observations of Bastian, Dulk, & Leblanc (2000), the VLSS offers the potential for obtaining multiple observations on a substantial fraction of the extrasolar planet census. (The limitation on the number of stars that can be observed by the VLSS is its southern declination limit of $-30°$. Thus, approximately one-third of the stars in the current census cannot be observed.) By observing a large number of stars, the VLSS has the potential for observing a rare, large burst.

Presently, the VLSS is 10% complete, having surveyed a a 0.9 sr region. As an illustration of its future utility as well as to confront the models with what limited observations may be available, we have examined the locations of the known extrasolar planets within the current survey region. Figure 2 shows the field around 70 Vir as a typical example.

In the current census, 5 stars fall within the region surveyed thus far. In no case have we detected emission at the location of an extrasolar planet. Table 2 summarizes the upper limits we derive; we reproduce the predicted emission frequencies and "burst" flux densities for convenience as well. We obtain the upper limits by determining the local noise level (σ), which is typically near 100 mJy. Radio sources in common to the 74 MHz VLSS and the 1400 MHz NVSS are used to register the positions of sources detected in VLSS, and experience shows that the reference frames at the two frequencies agree to within approximately $5''$. The radio reference frame provided by
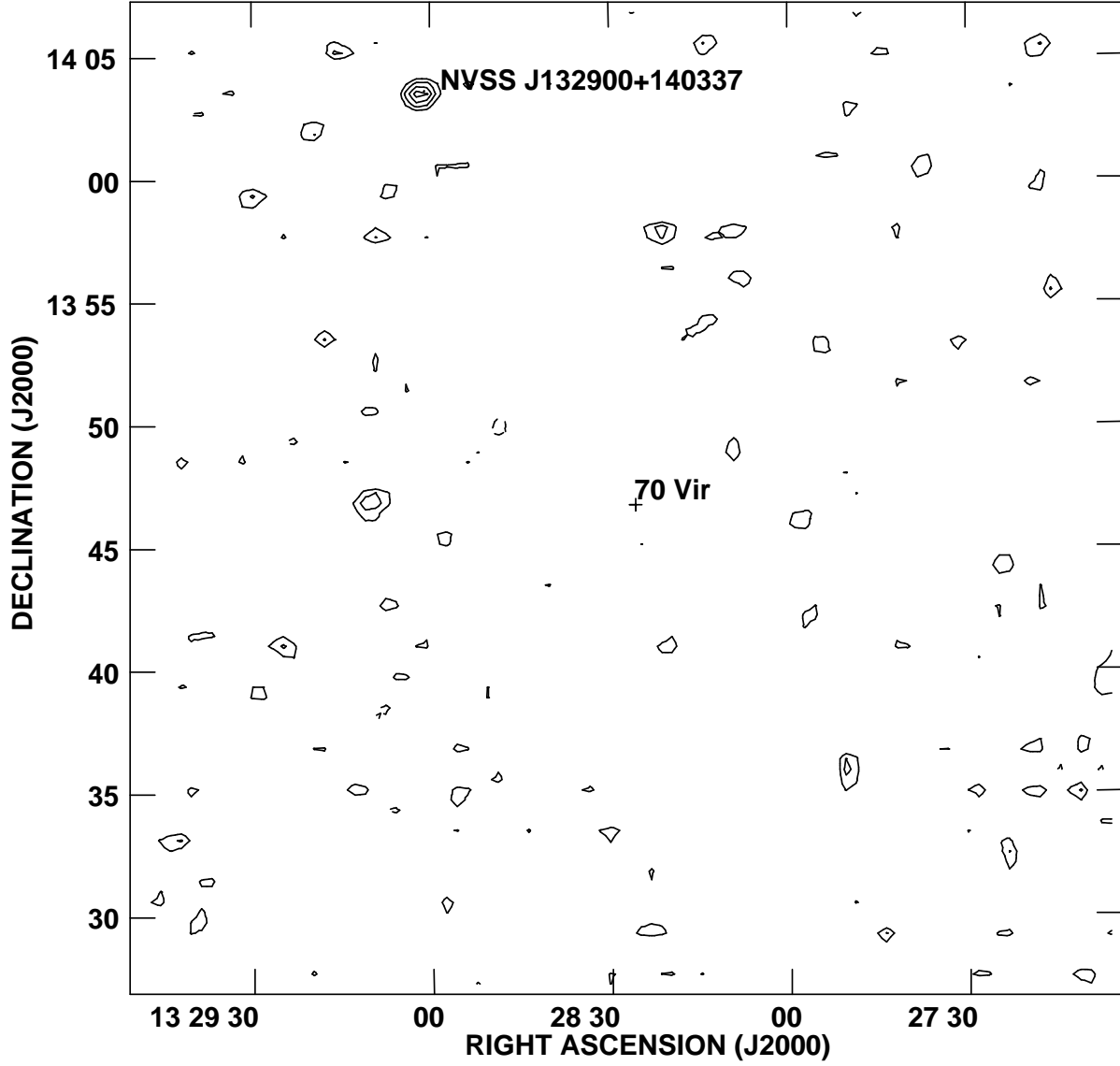
Fig. 2.— The field around 70 Vir at 74 MHz, illustrating the typical field observed in the VLSS. The noise level is 0.13 Jy beam^{-1}, with a $25'' \times 25''$ beam. The contours are 0.13 Jy beam$^{-1} \times$ $-3, 2, 3, 4, 5, 7.07$, and 10. The position of 70 Vir is marked by a cross. Also indicated is the radio source NVSS J132900+140337, likely to be an extragalactic radio source.

the NVSS itself should be aligned to within 40 milliarcseconds of the optical reference frame. Thus, the locations of the stars hosting extrasolar planets are known to a much better precision than the beam (point-spread function) of the VLA at 74 MHz (80″). As a result, we have adopted a signal-to-noise threshold of 2.5σ in setting upper limits.

Of the 5 extrasolar planets within the currently surveyed region of the VLSS, two have predicted emission frequencies well above the survey frequency of 74 MHz. On the basis of the model, we would not expect to see emission at the location of these stars. We emphasize, though, that one of our purposes in comparing the VLSS observations to the model predictions is an effort to confront the model with whatever observations are available.

For the remaining 3 extrasolar planets, their emission frequencies are all within nearly a factor of 2 of 74 MHz. In these cases we can explain the absence of emission as due to the low flux densities expected, though τ Boo is a possible exception. For τ Boo the observed upper limit is within a factor of only 3 of the expected "burst" emission levels. As Farrell et al. (1999) discussed, τ Boo remains a potentially useful target for further tests. (See also Farrell et al. 2003 for further observations of τ Boo.)

5. Discussions and Conclusions

We have used the extrasolar planet census, as of 2003 July 1, and scaling laws developed in our solar system to predict the emission frequencies and flux densities for radio emission from extrasolar planets. Our work presents an update and extension of the initial work of Farrell et al. (1999). Figure 1 and Table 1 present our primary results. Selection effects due to the current planet detection methodology produce an apparent deficit of planets with low flux densities and small emission frequencies. There is also a deficit of planets with high flux densities and large emission frequencies due to the well-known deficit of planets with both large masses and small semi-major axes.

The most likely planets to be detected are those orbiting nearby stars. Thus, the planet orbiting OGLE-TR-56 is similar to many of the other "close-in" planets, but its flux density is roughly 3 orders of magnitude lower than most of the other planets in the census because of its much greater distance (1500 pc vs. a more typical 10 pc). This result is likely to be a general result as future planetary searches move deeper into the Galaxy.

We have also used the initial observations of the 74 MHz VLA Low-frequency Sky Survey (VLSS) to place constraints on the emission from a small number of planets. In no case do we detect any emission, and the typical upper limit is approximately 0.3 Jy. For most of the planets, the predicted flux density is orders of magnitude lower than the upper limit, but the upper limit for the planet orbiting τ Boo is within a factor of 2 of the predicted "burst" flux density.

Most of the known extrasolar planets have expected emission frequencies below 1000 MHz. In-

deed, if equation (4) is correct, we do not expect extrasolar planets to emit strongly above 1000 MHz because their magnetic moments are not large enough. Thus, efforts to detect the radio emission from extrasolar planets must focus on the low-frequency capabilities of current or future radio telescopes.

In designing an experiment to detect extrasolar planets, the potential for bursts must be taken into account. The sensitivity of a radio telescope improves with increasing integration time as $t^{-1/2}$. Longer integration times improve the sensitivity but at the cost of "diluting" any bursts. For a burst of flux density S_b and duration Δt_b, its average flux density in an integration time t is $S_b(\Delta t_b/t)$, i.e., the burst is diluted with time as t^{-1}. To the extent that extrasolar planet radio emission is "bursty" (as is observed for the solar system planets), multiple short observations are a better strategy than long integrations, as are employed usually in radio astronomy.

We shall now estimate the sensitivity of various radio telescopes for detecting extrasolar planets. In estimating radio telescope sensitivities, particularly for aperture synthesis instruments, it is common to use long integration times ($\sim$ 8 hr). In contrast, the magnetospheres of the solar system planets respond to solar wind variations on time scales of order 1 hr. We shall use 15 min. as an integration time both to emphasize that long integration times may not be appropriate for estimating sensitivities and to allow for the possibility that shorter magnetosphere response times may occur.

The Very Large Array has been used already in attempts to detect radio emission from extrasolar planets (Bastian et al. 2000; Farrell et al. 2003), and as we illustrate here, its on-going 74 MHz northern sky survey provides an excellent opportunity to continue testing these models. Below 1000 MHz, the VLA operates at 74 and 330 MHz. Its nominal sensitivity at these two frequencies is roughly $200\,\mathrm{mJy}/\sqrt{t/15\,\mathrm{min.}}$ and $1.5\,\mathrm{mJy}/\sqrt{t/15\,\mathrm{min.}}$ over bandwidths of 1.5 and 3 MHz, respectively. As Figure 1 demonstrates, only if the radiometric Bode's Law vastly underestimates the radiated power levels will the VLA be able to detect radio emissions from extrasolar planets, even taking into account the possibility of strong bursts.

The Giant Metrewave Radio Telescope (GMRT) operates at frequencies of 150, 235, 330, and 610 MHz. Over this frequency range, its nominal sensitivity varies somewhat but is roughly $0.2\,\mathrm{mJy}/\sqrt{t/15\,\mathrm{min.}}$ in a 4-MHz bandwidth. Although larger bandwidths (and therefore improved sensitivities) are technically possible with the GMRT, we use a 4-MHz bandwidth in an attempt to strike a balance between improved sensitivity and avoiding terrestrially-generated radio interference. As Figure 1 shows, most extrasolar planets are below the detection limit of the GMRT, unless they produce strong bursts (factor of roughly 100 increase in flux density).

The Low Frequency Array (LOFAR) is a radio telescope in the design and development phase that is expected to operate in the frequency range 10–240 MHz. This frequency range encompasses the predicted emission frequencies of roughly two-thirds of the current census. The sensitivity of LOFAR will be highly frequency- and direction-dependent, due to the effect on the system temperature from the Galactic synchrotron emission. For directions away from the Galactic plane, the

design goals specify a sensitivity, in a 15-min. integration with a 4-MHz bandwidth, around 2 mJy at the lower frequencies and increasing to around 1 mJy at the higher frequencies. There are a number of potential candidates for observations with LOFAR. Perhaps most promising are τ Boo, Gl 876, and Gl 86 as these three objects may be detectable even in the absence of any flux density increase due to stellar wind variability. Also of interest are HD 162020 and HD 195019, which may require only moderate increases (factor of 10) due to stellar wind variability to become detectable.

The Square Kilometer Array (SKA) is a next-generation radio telescope that is expected to operate above 150 MHz. Its current design goals suggest that its sensitivity would be approximately 1 μJy in a 15-min. integration. This sensitivity is sufficient that it should be capable of detecting the radio emissions from the most massive extrasolar planets, without relying upon bursts to enhance the emission levels, and a substantial fraction of the current census if their burst levels are comparable to what we find here. The efficacy of the SKA in detecting the radio emission from extrasolar planets depends upon two aspects of its design, the lowest frequency at which it operates and its collecting area. First, if the potential SKA frequency range were to be increased to extend below 150 MHz, the number of planets it potentially could detect would also increase. Second, as stated currently, the SKA sensitivity is specified in terms of a ratio between its effective collecting area and system temperature, $A_{\mathrm{eff}}/T_{\mathrm{sys}}$. This quantity is taken to be constant. As T_{sys} increases below 1000 MHz due to Galactic synchrotron emission, this design goal requires that A_{eff} also increase below 1000 MHz so as to keep the ratio constant. If this design goal is relaxed so that $A_{\mathrm{eff}}/T_{\mathrm{sys}}$ decreases below 1000 MHz, the likelihood of the SKA detecting the radio emission from extrasolar planets also decreases.

All of our discussions assume that the radio emissions from these planets would be driven solely by the stellar wind loading of the planets' magnetospheres. If there are large, close-in satellites, like Io at Jupiter, higher emission frequencies and flux densities could result. Also, for planets in close to their parent stars, magnetic pressures that are large in the interior heliosphere may drive radio emission (Zarka et al. 2003). Future modeling efforts include integrating the current census with these hot Jupiter emission models.

REFERENCES

Barrow, C. H., Genova, F., & Desch, M. D. 1986, A&A, 165, 244

Bastian, T. S., Dulk, G. A., & Leblanc, Y. 2000, ApJ, 545, 1058

Berger, E., Ball, S., Becker, K. M., et al. 2001, Nature, 410, 338

Blackett, P. M. S. 1947, Nature, 159, 658

Butler, P., Vogt, S., Marcy, G., Fischer, D., Henry, G., & Apps, K. 2000 ApJ, 545, 504

Butler, P., Marcy, G., Fischer, D., Brown, T., Contos, A., Korzennik, S., Nisenson, P., & Noyes, R. 1999 ApJ, 526, 916

Chapman, S. & Ferraro, V. C. A. 1932, Terr. Magn. Atmos. Electr., 37, 421

Chapman, S. & Ferraro, V. C. A. 1931, Terr. Magn. Atmos. Electr., 36, 77

Charbonneau, D., Brown, T. M., Noyes, R. W., & Gilliland, R. L. 2002, ApJ, 568, 377

Desch, M. D. 1988, Geophys. Res. Lett., 15, 114

Desch, M. D. & Rucker, H. O. 1985, AdSpR, 5, 333

Desch, M. D. & Barrow, C. H. 1984, J. Geophys. Res., 89, 6819

Desch, M. D. & Kaiser, M. L. 1984, Nature, 310, 755

Farrell, W. M., Lazio, T. J. W., Desch, M. D., Bastian, T., & Zarka, P. 2003, in Bioastronomy 2002: Life Among the Stars, eds. R. Norris, C. Oliver, & F. Stootman (ASP: San Francisco) in press

Farrell, W. M., Desch, M. D., & Zarka, P. 1999, J. Geophys. Res., 104, 14025

Fischer, D., Marcy, G., Butler, P., Vogt, S., Frink, S., & Apps, K. 2001, ApJ, 551, 1107

Gallagher, D. L. & D'angelo, N. 1981, Geophys. Res. Lett., 8, 1087

Goldreich, P. & Soter, S. 1966, Icarus, 5, 375

Guillot, T., Burrows, A., Hubbard, W. B., Lunine, J. I., & Saumon, D. 1996, ApJ, 459, L35

Gurnett, D. A. 1974, J. Geophys. Res., 79, 4227

Han, I., Black, D. C., & Gatewood, G. 2001, ApJ, 548, L57

Henry, G. W., Donahue, R. A., & Baliunas, S. L. 2002, ApJ, 577, L111

Jones, H. R. A., Butler, R. P., Marcy, G. W., Tinney, C. G., Penny, A. J., McCarthy, C., & Carter, B. D. 2002, MNRAS, 337, 1170

Kassim, N. E., et al. 2003, ApJS, in press

Lecacheux, A. 1991, in Bioastronomy The Exploration Broadens, Proceedings of the Third International Symposium on Bio-astronomy, eds. J. Heidmann & M. J. Klein (Springer-Verlag: Berlin) p. 21

Lecacheux, A., Zarka, P., Desch, M. D., & Evans, D. R. 1993, Geophys. Res. Lett., 20, 2711

Konacki, M., Torres, G., Jha, S., & Sasselov, D. D. 2003, Nature, 421, 507

Marcy, G. W. 2003, in Bioastronomy 2002: Life Among the Stars, eds. R. Norris, C. Oliver, & F. Stootman (Astron. Soc. Pacific: San Francisco) in press

Mazeh, T., Zucker, S., dalla Torre, A., & van Leeuwen, F. 1999, ApJ, 522, L149

Millon, M. A. & Goertz, C. K. 1988, Geophys. Res. Lett., 15, 111

Mitchell, D. L., Lin, R. P., Mazelle, C., et al. 2001, J. Geophys. Res.-Planets, 106, 23419

Quillen, A. C., & Thorndike, S. 2002, ApJ, 578, L149

Rucker, H. O. 1987, Annales Geophysicae, Series A, 5, 1

Santos, N. C., Udry, S., Mayor, M., et al. 2003, A&A, 406, 373

Schneider, J. 2003, "Extrasolar Planets Encyclopaedia," http://www.obspm.fr/encycl/encycl.html

Setiawan, J., Hatzes, A. P., von der Lühe, O., et al. 2003, A&A, 398, L19

Shkolnik, E., Walker, G. A. H., & Bohlender, D. A. 2003, ApJ, 597, 1092

Trilling, D. E. 2000, ApJ, 537, L61

Udry, S., Mayor, M., & Queloz, D. 2000, in Planetary Systems in the Universe: Observation, Formation, and Evolution, eds. A. Penny, P. Artymowicz, A.-M. Lagrange, & S. Russell (ASP: San Francisco)

Vogt, S., Marcy, G., Butler, P., & Apps, K., 1999 ApJ, 536, 902

Wu, C. S. & Lee, L. C. 1979, ApJ, 230, 621

Yantis, W. F., Sullivan, W. T., III, & Erickson, W. C. 1977, BAAS, 9, 453

Zarka, P., et al. 2003, Planetary Space Sci., in press

Zarka, P., Treumann, R. A., Ryabov, B. P., & Ryabov, V. B. 2001, Ap&SS, 277, 293

Zarka, P., et al. 1997, in Planetary Radio Astronomy IV, eds. H. O. Rucker, S. J. Bauer, & A. Lecacheux (Austrian Acad. Sci. Press: Vienna) p. 101

Table 2.   74 MHz VLSS Constraints on Extrasolar Planetary Radio Emission

Star	ν_c (MHz)	S_{model} (mJy)	S_{observe} (mJy)
HD 104985	505	0.03	220
HD 108874	54	0.06	325
70 Vir	546	1.6	325
τ Boo	60	100	275
ρ CrB	28	16	218

Note. — The model flux densities are the "burst" flux densities, obtained by multiplying the median levels predicted by equation (3) by a factor of 100. The upper limits given by S_{observe} are 2.5σ in the VLSS 74 MHz images.